UCRL-11155
c.2

University of California

Ernest O. Lawrence Radiation Laboratory

TWO-WEEK LOAN COPY

This is a Library Circulating Copy
which may be borrowed for two weeks.
For a personal retention copy, call
Tech. Info. Division, Ext. 5545

K^-p ELASTIC SCATTERING AT 1.22 BeV/c

Berkeley, California

UCRL-11155
c.2

DISCLAIMER

This document was prepared as an account of work sponsored by the United States Government. While this document is believed to contain correct information, neither the United States Government nor any agency thereof, nor the Regents of the University of California, nor any of their employees, makes any warranty, express or implied, or assumes any legal responsibility for the accuracy, completeness, or usefulness of any information, apparatus, product, or process disclosed, or represents that its use would not infringe privately owned rights. Reference herein to any specific commercial product, process, or service by its trade name, trademark, manufacturer, or otherwise, does not necessarily constitute or imply its endorsement, recommendation, or favoring by the United States Government or any agency thereof, or the Regents of the University of California. The views and opinions of authors expressed herein do not necessarily state or reflect those of the United States Government or any agency thereof or the Regents of the University of California.

UCRL-11155
UC-34 Physics
TID-4500 (24th Ed.)

UNIVERSITY OF CALIFORNIA
Lawrence Radiation Laboratory
Berkeley, California

AEC Contract No. W-7405-eng-48

K^-p ELASTIC SCATTERING AT 1.22 BeV/c

John H. Munson

(Ph. D. Thesis, Part II)

December 20, 1963

Printed in USA. Price $1.00. Available from the
Office of Technical Services
U. S. Department of Commerce
Washington 25, D.C.

K^-p ELASTIC SCATTERING AT 1.22 BeV/c

Contents

Abstract v

I. Introduction 1

II. Data Acquisition and Data Processing

A. The Beam 2

B. Scanning and Measuring 2

C. Computer Analysis 3

III. Treatment of the Data

A. Path Lengths 6

B. Size of the Processed Portion of the Sample . . 8

C. Possible Reactions and Ambiguities 9

D. Corrections to the Angular Distribution and Fitting 17

IV. Discussion 22

Acknowledgments 30

References 31

K^-p ELASTIC SCATTERING AT 1.22 BeV/c

John H. Munson

Lawrence Radiation Laboratory
University of California
Berkeley, California

December 6, 1963

ABSTRACT

Three thousand K^-p elastic scatterings at 1.22 BeV/c have been studied. These events are part of a sample of 7000 events of the "two-prong" topology, produced in the Lawrence Radiation Laboratory 72-inch hydrogen bubble chamber, and measured on the new Scanning and Measuring Projectors of the Alvarez group. Fitting of the corrected elastic-scattering center-of-mass angular distribution suggests that terms to $\cos^6\theta$ are needed, although a fit to $\cos^5\theta$ is certainly not excluded. The elastic-scattering data, together with the published charge-exchange data from the same exposure and data at 1.34 BeV/c, are subjected to a partial-wave analysis, parameterized in terms of K^-p resonances at 1765, 1815, and 2100 MeV. (The $Y_0^*(2100)$ parameterization, with width 180 MeV and elasticity 0.35, is suggested by the K^-p and K^-n total-cross-section curves.) The predicted angular distributions are in good agreement with the experimental distributions. Dalitz plots are presented for the partially analyzed three-body reactions appearing in the two-prong topology, and obtained as a by-product.

I. INTRODUCTION

In the summer of 1963, 7000 K^- events in a hydrogen bubble chamber were measured and analyzed in an experiment with a twofold purpose: to determine the K^-p elastic-scattering cross section at 1.22 BeV/c incident K^- momentum; and to initiate the new Scanning and Measuring Projectors (SMP's) into the Alvarez group data-analysis system.

For the "SMP shakedown" aspect of the experiment, it was desirable to employ a set of plentiful events, which had a simple topology and were highly overdetermined by kinematic constraints. The obvious candidates were elastic scatterings. The measurement and analysis of a sample of elastic scatterings allowed the simplest direct examination of the operation of the SMP's. The elastic scatterings are found in the "two-prong," or Y-shaped, topology, of which there was a copious supply on the 1.22-BeV/c K^- film. This film also had a relatively low flux of incident beam tracks, which facilitated the scanning for events and the analysis of the SMP performance.

A special interest in the elastic scattering at 1.22 BeV/c was a concurring factor in the choice of the set of events to be analyzed. The published charge-exchange differential cross section at this momentum (indeed, from the same film) exhibits a large backward peak and requires a fit to $\cos^6\theta$ (c.m.). Knowledge of the elastic scattering was needed to further our understanding of this interesting phenomenon.

In Sec. II, we discuss the acquisition and computer analysis of the data. Section III describes the separation of the three-body events from the elastic scattering, the corrections applied to the elastic-scattering data, and the results obtained in power-series fits. Finally, in Sec. IV, we examine the elastic and charge-exchange data, as well as other relevant data, in the light of a partial-wave analysis and a suggested set of partial-wave amplitudes.

II. DATA ACQUISITION AND DATA PROCESSING

A. The Beam

In 1961 and 1962, the Alvarez 72-inch hydrogen bubble chamber at the Lawrence Radiation Laboratory was exposed to a two-stage separated K^- beam, in a series of experiments often called collectively the "K-72 experiment."[1] The K^- beam was designed and constructed under the supervision of Dr. Harold K. Ticho. The beam was introduced to the bubble chamber at eight different momenta, from 1.0 to 1.7 BeV/c. The film at 1.22 BeV/c was chosen for the present experiment, for reasons outlined in Sec. I. At this momentum setting, the momentum spread of the beam was approximately ±40 MeV/c.

Of the 133 rolls of film (80,000 frames) exposed at 1.22 BeV/c, approximately 58 rolls were measured in this experiment. In a partial scan spread across the 58 rolls, we found 3.8 beam tracks (and 0.95 interaction and decay) per frame. These figures include both K^- and contaminant particles. The composition of the beam is discussed in Sec. III. A.

B. Scanning and Measuring

Although the film used in this experiment had been scanned for more complex topologies in the course of the K-72 experiment, the two-prong events at 1.22 BeV/c were not recorded. Therefore, a scan and rescan of the film were done specifically for this experiment. The scanning intructions were simple: to record all two-prong interactions, except those with associated V's or in which one of the prongs decayed. Events with these extra features were previously measured and analyzed in the K-72 experiment. Other secondary interactions or decays of the product particles do not affect the two-prong classification of the primary interaction. Thus, the only class of elastic scatterings omitted in the scanning were those in which the outgoing K^- suffered a one-prong decay in the chamber. The number of these events is negligible within the statistics of our experiment, since even the slowest K^-

mesons are more likely to interact in the chamber than to decay. The scanning instructions also included the typical restrictions against events lying outside a fiducial region, and against obviously nonbeam incident tracks.

Rescan of the film indicated an efficiency of 98% in the first scan. The events found in the rescan were not measured. Since the omissions in scanning such simple event topologies generally contain a large proportion of "obvious" events overlooked, the omitted events are not felt to be highly biased as to configuration. The corrections involved with scanning efficiency are discussed further in Sec. III. B.

Approximately 7000 events were measured, and failing events remeasured, on the SMP's from April 29 to July 30, 1963. Part I of the author's thesis fully describes the SMP machines and system,[2] which are discussed here only in the few points relevant to this experiment. The film was scanned on conventional scanning tables rather than on the SMP's, for economic reasons discussed in Ref. 2. We began with one SMP measuring for approximately 40 hours per week, under the close scrutiny of physicists. At the close of measuring, two SMP's were each being manned approximately 130 hours per week. During this period, the SMP's were found to operate with consistency and accuracy on a par with the group's digitized projection microscopes. By the end of the measuring period, the SMP's demanded the experimenter's attention only occasionally.

The measuring of the film for this experiment was arbitrarily terminated after 58 rolls, with the advent of new film from the Alvarez group 1963-1964 K and π experiment complexes. After completing the remeasurements on the two-prong film, the SMP's were entered into the new experiments.

C. Computer Analysis

Figure 1 shows the analysis chain through which the events passed. All the rectangular blocks represent computer programs. The use of these programs has become standard in the Alvarez group.[3]

The SMP program is an IBM 709 program written by the author and others at the Radiation Laboratory for controlling the SMP measurements and preparing the measurement data in a form suitable for injection into the existing analysis system.[2] To speed the introduction of the SMP's into the Alvarez-group system, the computer program was designed to allow the SMP's to be fully interchangeable with the existing digitized projection microscopes. The data analysis and the clerical data-handling procedures for the entire experiment, in fact, were treated as a pilot model for the succeeding large K and π experiments, which use both the SMP's and the projection microscopes.

Computer programs other than the SMP program were run on the Radiation Laboratory's IBM 7090 computer. LINGO is a library program that maintains a complete file showing the progress of each event in the experiment. (This file is the Master List tape, ML.) Throughout the analysis, LINGO performs a variety of services, updating, tallying, and listing data. Such a computerized "inventory control" is becoming a necessity for today's large experiments.

The other programs constitute the standard chain of analysis in the Alvarez group, representing the typical steps in event analysis. The flow chart reflects one recent change in the processing of events: the EXAMIN-type program DST EXAM II has been placed after the "intersection" at which measurement results are returned to the library. This procedure has the important advantage that the DST EXAM II program may be modified at will to calculate new quantities of physical interest, without disturbing the format and operation of the library program. As shown, however, the system has a drawback. The DST EXAM II program may reject an event considered passing by LINGO. Feedback from beyond the DST EXAM II program should be arranged, to allow the library to request remeasurements of such events.

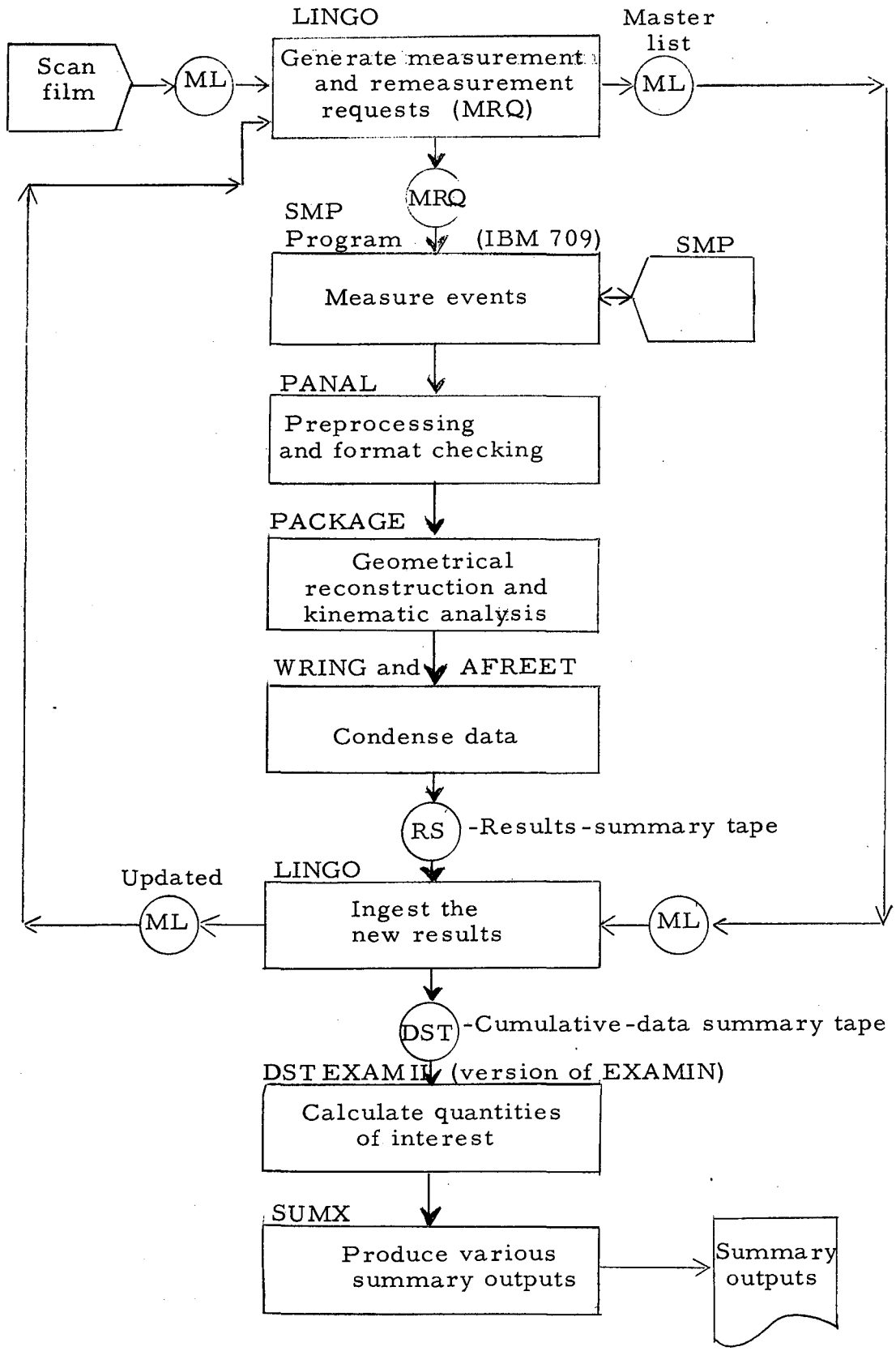

Fig. 1. The data-analysis system for the two-prong experiment

III. TREATMENT OF THE DATA

A. Path Lengths

The K^- path length in the measured sample of 58 rolls (hereafter called the "sample") was determined by counting the τ decays,

$$K^- \rightarrow \pi^-\pi^+\pi^- ,$$

which were scanned twice as part of the K-72 experiment. The better-controlled scan, which we call Scan A, found 936 events in the sample. Scan B found 47 events not on Scan A. All these 47 events, and some found on Scan A but not on Scan B, were reexamined on the scanning table; 28 of the 47 events were actually π's.

The scanning situation is complicated by the presence of false τ decays appearing in the reactions

$$K^- \rightarrow \left\{ \begin{array}{l} \pi^-\pi^0 \\ \mu^-\bar{\nu}\pi^0 \\ e^-\bar{\nu}\pi^0 \\ \pi^-\pi^0\pi^0 \end{array} \right\} ; \pi^0 \rightarrow 2\gamma; \gamma \rightarrow e^+e^- .$$

The various branching ratios determine that the ratio of false τ decays to true τ decays is 7%.[4] Some fraction of the false τ decays is detectable on the scanning table, owing to their wider possible opening angle and the visible presence of Dalitz electron pairs. In the imperfectly controlled K-72 scanning, visibly false τ's were variously included in the τ's, omitted, or "flagged" by the scanner as false τ's. If all false τ's had been recorded, we could have simply counted them with the τ's in determining the K^- path length, using the combined branching ratio. Events flagged by the scanner in Scan A amounted to 4% of the total, a reasonable proportion of the 7% false τ decays.

We note that a few τ decays should be missed because they are hard to see (the negative tracks may overlap closely, or other tracks in the frame may interfere). The statistical loss in the double scan amounts to less than one event. Finally, the τ decays are assumed to be scanned under the same fiducial-volume criteria as the two-prong events. Then, we calculate:

936	τ and false τ decays found on Scan A
+28	τ's found on B, not A
-21	improperly listed events on A (11 found, 10 estimated)
-58	false τ's on A (38 flagged, 20 estimated)
+10	estimated hard-to-scan τ decays
= 895	estimated τ decays in our sample.

The errors in the corrections are less than the ±3% statistical error in the number of τ events. Incorporating a K^- half-life of 1.22×10^{-8} sec, and a τ-decay branching ratio of (5.72±0.17)%,[4] we find a K^- path length of $(14.2\pm0.6)\times10^6$ cm in the sample, corresponding to a yield of (504±23) events/mb.

The π path length was found by two independent methods. First, 12 "associated production" events of the type $\pi^-p \rightarrow K^0\Lambda^0$ had been found in the complete 1.22-BeV/c film. Using a factor of 9/2 for detection efficiency and a cross section of 0.53 mb, we found the π^- path length (in the sample only) to be $(1.2\pm0.4)\times10^6$ cm, or (43±14) events/mb.

Second, approximately a quarter of the measured two-prong events were processed through a PACKAGE program that tested the π^-p elastic scattering hypothesis. In the forward directions (in the center-of-mass system), π^-p and K^-p elastic scatterings are hard to distinguish. But in the backward hemisphere, the kinematic separation is clean, and 15 events were found to be unambiguous π^-p elastic scatterings. Only two poorly measured events fitted both the K^-p and π^-p hypotheses. These two were probably K's, a priori.

The π elastic-scattering cross section in the backward hemisphere at 1.22 BeV/c was interpolated from published differential cross sections.[5] The figure (3 mb) and the number of events (15), scaled up to the full sample, yielded a π path length identical to that from the associated-production events: $(1.2\pm0.4)\times10^6$ cm. Because of the difficulties in scaling the two determinations, we avoid combining the two to reduce the statistical error.

For completeness, the total path length of all beam particles was estimated by counting the beam tracks entering and leaving a subsample of the film frames. It was planned to scale up the path length of beam

tracks (averaged over the length of the chamber) by the ratio of the numbers of frames in the subsample and the sample. The incident flux varied so greatly throughout the sample, however, that the subsample was not representative. Therefore, the beam path length was scaled instead by the ratio of the numbers of two-prong events in the subsample and the sample. (This normalization is inaccurate only to the extent that the proportion of noninteracting particles in the beam-μ's and electrons-is not representative in the subsample.) Using this normalization, we found a total path length of $(19.9 \pm 1.2) \times 10^6$ cm in the sample.

These determinations show the beam to be composed of approximately 70% K's, 6% π's, and 24% leptons. The ratio of π path length to K path length is approximately 8%.

Because both the entering and leaving beam tracks were counted in the total path-length scan, the number of particles removed from the beam could be compared with the removals expected due to K and π interactions and decays. This check was well satisfied, although it was of limited significance, owing to statistical errors in sample sizes and uncertainties in scaling factors.

B. Size of the Processed Portion of the Sample

An absolute cross-section determination was one goal of this experiment. Determining the cross section necessitated the study of path lengths just described, and also the evaluation of the percentage of sample events that were actually measured and processed. The scan list for the sample contained 10,945 events. The rescan indicated that about 200 more events should be added, but the SMP operators (who presumably must look at the events more carefully than the scanners) rejected a comparable number of events as not being two-prongs.

Only some 7000 events were measured, of the more than 10,000 events in the sample. The remaining events were rejected by the SMP operators for a variety of reasons. The two primary reasons for rejection were specific to the SMP shakedown procedure: events were rejected if the interaction vertex was too near another beam track or

outside a restricted region in the bubble chamber. Events were also rejected if they were unmeasurable for various reasons.

The frequency of these "operator rejects" is independent of the configuration of the event, so the effect of the rejections on the cross sections may be described by a single multiplicative constant. We now claim that the same essentially holds for the events failing in the PANAL and PACKAGE programs, and those failing further fiducial and beam criteria in DST EXAM II. The PANAL and PACKAGE failures are largely configuration-independent because they depend on individual tracks or on gross measurement errors. (Besides, the failing events were remeasured, eliminating all but a doubly reduced number of residual PANAL and PACKAGE failures.)

In short, we describe all the causes of rejection with a single multiplicative factor. (The problem of remeasurements, the difficulties of our infant library and data-handling system, and the multitude of decision levels in the computer programs all make it difficult to reconstruct the correction in any greater detail.) The cumulative result of all the corrections is that the number of events in a given processed distribution should be multiplied by a factor of 1.75 to bring it into correspondence with the sample K path length derived from the 895 τ decays.

C. Possible Reactions and Ambiguities

At 1.22 BeV/c K^- momentum, the K-p system has an invariant mass of 1895 MeV/c^2. All strong interactions must produce products with total baryon number 1 and strangeness -1; at this mass the only possibilities are $\bar{K}N$, $\Lambda\pi$, $\Sigma\pi$, and ΞK, with possible additional π's. Among these reactions, the ones that will appear as two-prongs in the bubble chamber more than very rarely are

$$K^-p \rightarrow K^-p, \tag{1}$$

$$K^-p \rightarrow K^-p\pi^0, \tag{2}$$

$$K^-p \rightarrow K^-\pi^+n, \tag{3}$$

$$K^-p \rightarrow \pi^-p\bar{K}^0, \tag{4}$$

$$K^-p \rightarrow \pi^-\pi^+\Lambda^0, \tag{5}$$

$$K^-p \rightarrow \pi^-\pi^+\Sigma^0;\ \Sigma^0 \rightarrow \Lambda^0\gamma, \tag{6}$$

and reactions derived from Reaction (2) through (6) by the addition of π^0's, as permitted by the invariant mass. Accordingly, the PACKAGE program analyzing the two-prongs tested as hypotheses the six reactions above. PACKAGE also tested the four underconstrained "missing mass" hypotheses using the charged products in Reactions (2) through (5) and undetermined neutral products.

Others in the Alvarez group had already studied Reactions (4) through (6) in the same film sample in the K-72 experiment, using events with a charged decay of the $\bar{K}^0$ or Λ^0.

Since all products of the elastic-scattering Reaction (1) are visible, the reaction has the maximum overdetermination possible at a single vertex (four constraints). The three-body Reactions (2) through (6), however, have only one constraint. As a result, the computer analysis achieved a high degree of separation of Reaction (1) from the others, whereas there was a large measure of ambiguity among the three-body reactions. Of the approximately 2200 events that fitted best as three-body reactions, two thirds also fitted another three-body reaction.

Because of the large mass difference between π^+ and proton, the ambiguities between Reactions (1), (2), and (4) and (3), (5), and (6) could usually be resolved by examining the ionization of the positive track. Reactions (3), (5), and (6) occurred together ambiguously with high frequency. Accordingly, it was decided to look at only those ambiguous events involving any of the Reactions (1), (2), or (4). The author examined approximately 1000 such events on the scanning table. In the majority of cases, the ambiguities were resolved, and the identity of the reaction was entered into the DST EXAM II program. Table I displays the number of unambiguous and ambiguous reactions before and after this partial removal of ambiguities.

Dalitz plots for Reactions (2) through (6) after the removal of ambiguities are presented in Figures 2 through 6. Considerable proportions of ambiguous events remain; Reaction (2), for example, remains 25% ambiguous. For this reason, and because Reactions (4) through (6) have been previously investigated, the analysis of Reactions (2) through (6) has not been carried further. The three-body plots are shown for reference, as a by-product of the elastic-scattering investigation.

Table I. Unambiguous and ambiguous reactions before and after the partial removal of ambiguities.

Best hypothesis	Before removal (DST 2908)		After removal (DST 2909)	
	Unambiguous	Ambiguous	Unambiguous	Ambiguous
1	3147	79	3240	13
2	203	231	358	109
3	163	362	203	301
4	166	274	376	81
5	164	358	216	283
6	38	225	56	186

As noted above, the relatively few ambiguous events involving the important elastic scattering Reaction (1) were also examined. Almost without exception, these events were found to be elastic scatterings. In the great majority of cases, the other reaction involved was Reaction (3), which was fitted owing to a mismatch (since corrected) between the SMP and PANAL programs. Measured tracks were improperly marked as stopping, giving them the wrong momentum assignment. These events improperly maked as ambiguous were transferred back to Reaction (1) by using DST EXAM II. The events outside the "allowed" kinematic region on the Dalitz plot for Reaction (3) (Fig. 3) represent a similar collection of mistreated elastic scattering events. These events fitted only Reaction (3) in PACKAGE, and thus there was no fitted information for Reaction (1), to single out in DST EXAM II. These events lie in the far forward scattering angles. In the correction for scanning bias discussed in the following section, we compensate for their loss from the elastic-scattering distribution.

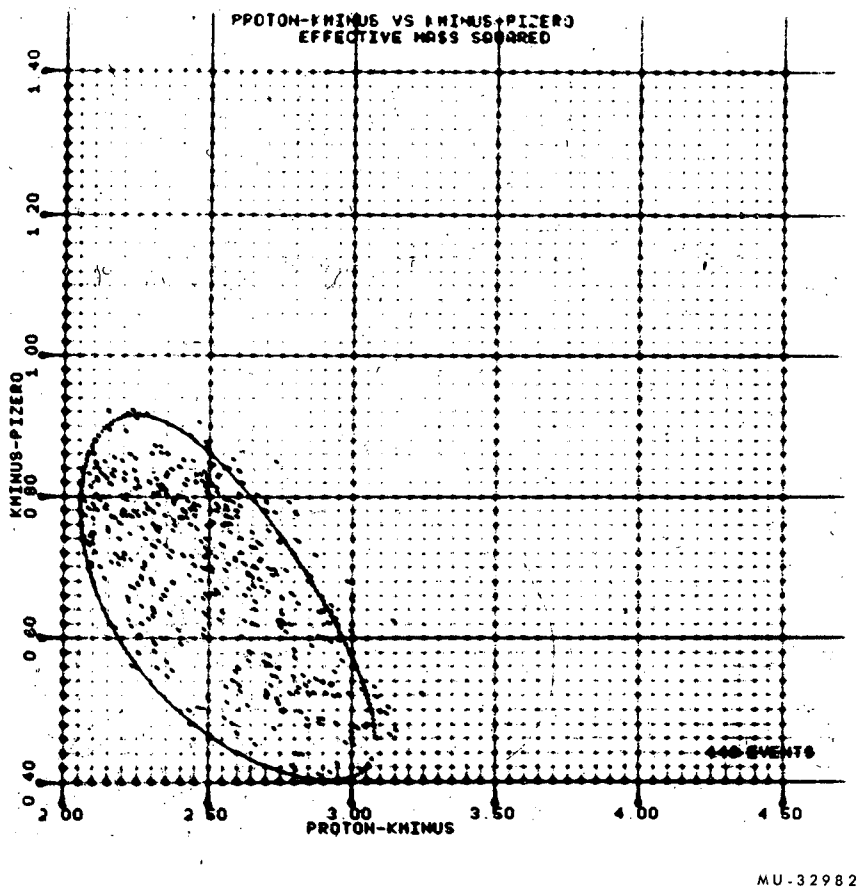

Fig. 2. Dalitz plot of the $K^-p\pi^0$ system.

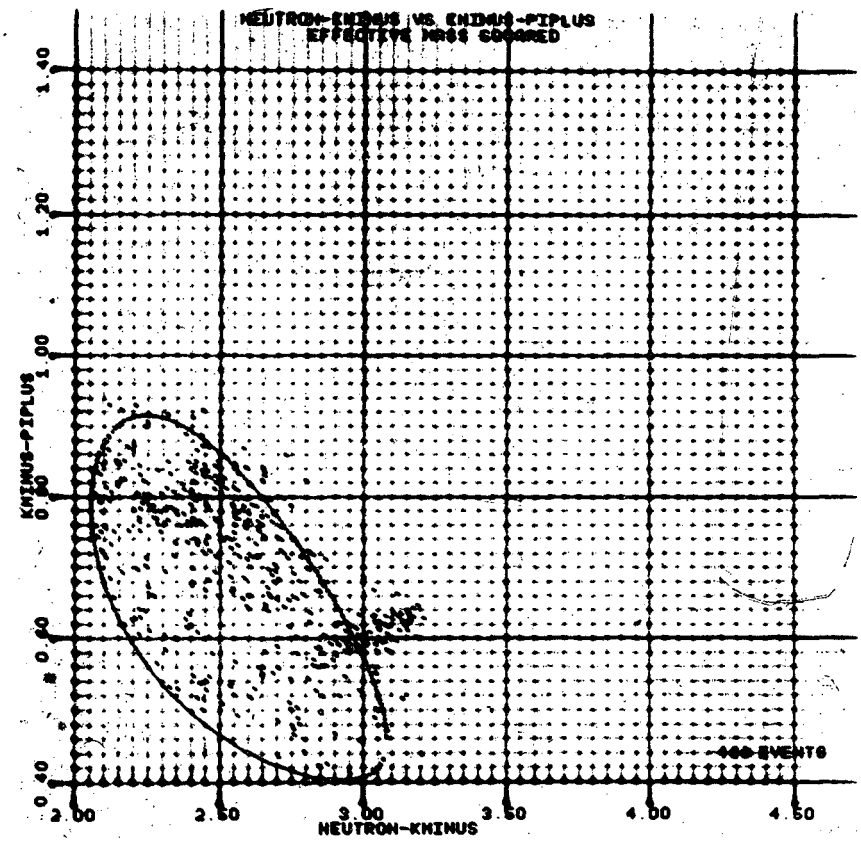

Fig. 3. Dalitz plot of the $K^-\pi^+n$ system.

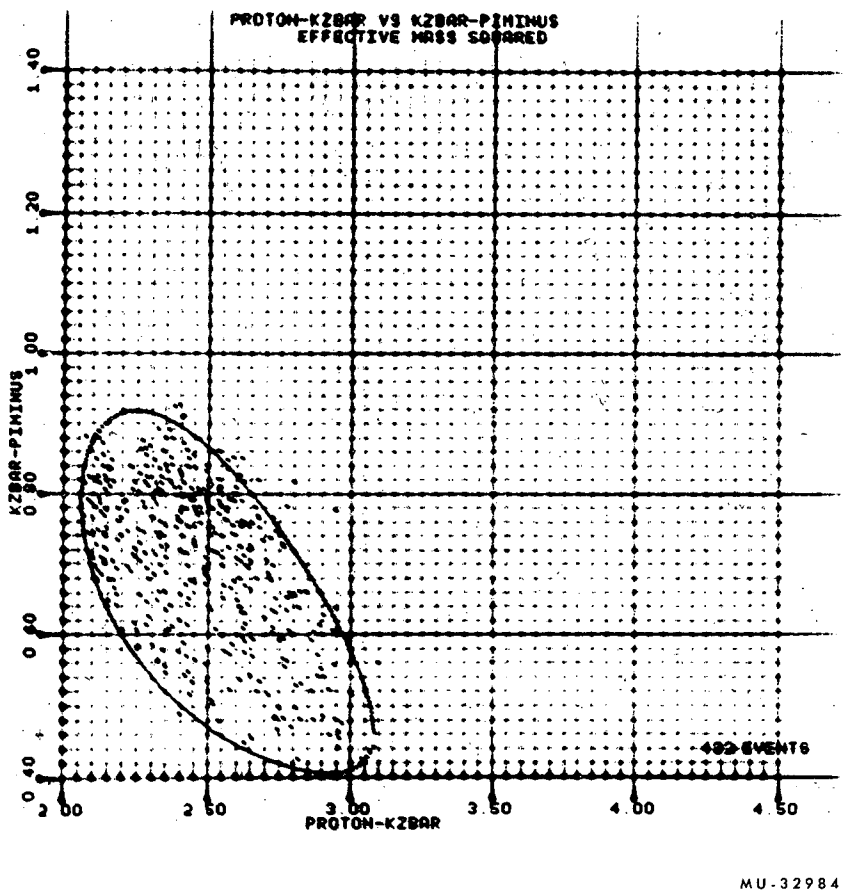

Fig. 4. Dalitz plot of the $\pi^- p \overline{K^0}$ system.

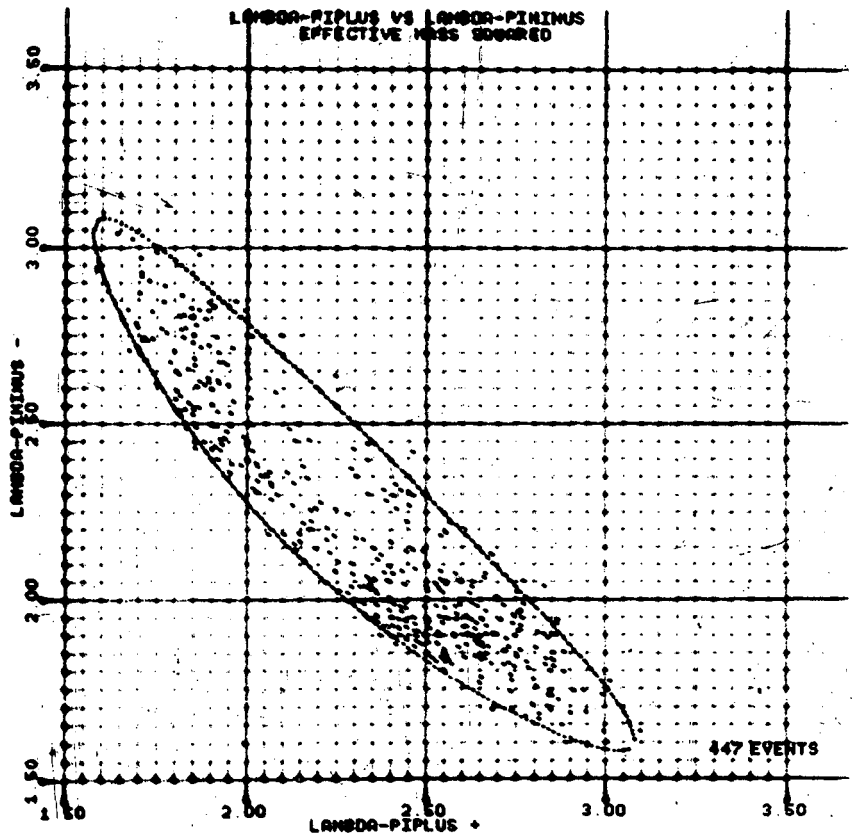

MU-32985

Fig. 5. Dalitz plot of the $\pi^-\pi^+\Lambda^0$ system.

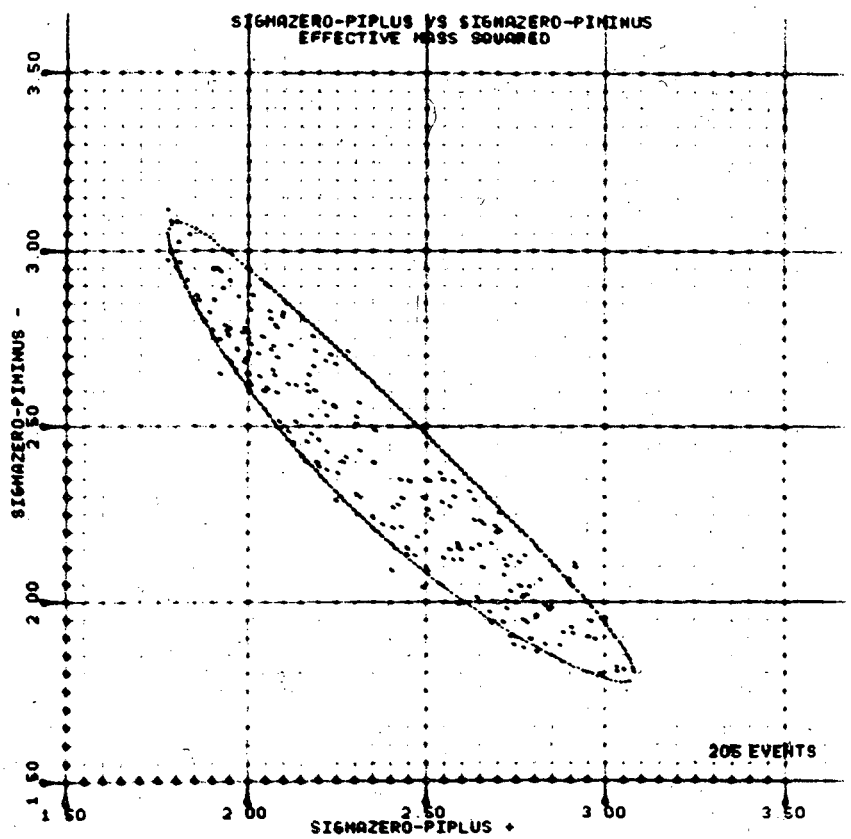

MU-32986

Fig. 6. Dalitz plot of the $\pi^-\pi^+\Sigma^0$ system.

D. Corrections to the Angular Distribution and Fitting

The observed elastic-scattering angular distribution was corrected for scanning efficiency at small angles, and for events arising from the π contamination. The correction for secondary K's that decay in the chamber and are rejected in the scanning was considered, but is negligible for the statistics of this experiment. Both the decay probability and the interaction probability obey a v^{-1} law at low momenta, and the interaction probability dominates throughout. Finally, the overall multiplicative factor discussed earlier was applied.

For small-angle scattering in the center-of-mass system ($\cos\theta > 0.9$), there is a severe depletion of events because of losses in scanning. The length of the recoil proton track and the change in K^- direction both become too small to see with certainty. Accordingly, this forward-angle region was omitted from the data used in the distribution to be fitted. By taking a two-dimensional histogram against both $\cos\theta$ and the orientation of the events about the beam track, we found a further depletion of forward scatterings in near-vertical scattering planes in the bubble chamber. This depletion is due to the same scanning bias; the vertical alignment of the event reduces the visible proton-track length and scattering angle in the stereo views. A correction was applied in the region ($0.7 \leq \cos\theta \leq 0.9$) by deleting the events aligned within 36° of the vertical, and upscaling the remaining distribution on the basis of azimuthal symmetry.

The $\pi^- p$ elastic scattering cross section is comparable in magnitude and angular distribution to that of $K^- p$, and the kinematic configuration of the two is very similar in the forward-scattering hemisphere. Therefore, events from the 8% π contamination will appear in the K distribution. At each scattering angle θ, the PACKAGE program will fit a certain fraction of π scatterings as K's, and will fit the same fraction of K scatterings as π's. It is possible to estimate this "faking function" of θ by examining the PACKAGE results for both the K and π elastic-scattering hypotheses on the same set of events. (The π- hypothesis PACKAGE was run to determine the π path length,

as was discussed previously.) Since most of the elastic scatterings are indeed K's, the ratio of events fitting as π's to those fitting as K's is essentially the faking function. The function we used is 1.0 for $\cos\theta > 0.6$ and drops linearly to 0.0 for $\cos\theta < 0.4$.

The π path length and the π elastic-scattering differential cross section at 1.22 BeV/c (interpolated from published values)[5] were used to obtain the π angular distribution. This distribution was then multiplied by the faking function, and subtracted from the K angular distribution.

After application of the corrections described above, the angular distribution shown in Fig. 7 was obtained. Power-series expansions of the angular distribution in the form

$$\frac{d\sigma}{d\Omega} = \frac{\lambda^2}{4} \sum_{n=0}^{N} A_n \cos^n \theta \qquad (7)$$

were fitted to the corrected distribution, using the general least-squares fitting program DJINN.[6] {The factor of 4 is included to account for the isotopic-spin decomposition of the K^-p amplitude: $(K^-p \mid K^-p) = 1/4\,[(1|1) + (1|0) + (0|1) + (0|0)]$.} Table II lists the goodness-of-fit parameters as a function of the order of the fits, N. The goodness of fit achieves a reasonable value at N = 5, increases at N = 6, and does not increase thereafter. The change from N = 5 to N = 6 corresponds to the fact that the fitted coefficient A_6 for N = 6 is more than two standard deviations away from zero. We conclude that N = 6 is probably needed to fit the data, although N = 5 is certainly not excluded. The coefficients of the fits for N = 5 and N = 6 are shown in Table III. These coefficients include a final scaling factor of 1.1, to account for high χ^2 elastic scatterings rejected by the DST EXAM II program. The data were also fitted with varying amounts of π contamination included, without significantly changing the results.

The fitted curves yield forward-scattering intensities $(d\sigma/d\Omega)_{\theta=0}$ of (8.0±0.8) mb/sr for N = 5 and (6.7±0.7 mb/sr for N = 6. The optical theorem predicts a minimum of 6.9 mb/sr, in agreement with either value. The curves yield total elastic cross section of (16.8±1.0)mb for N = 5 and (13.0±0.8) for N = 6.

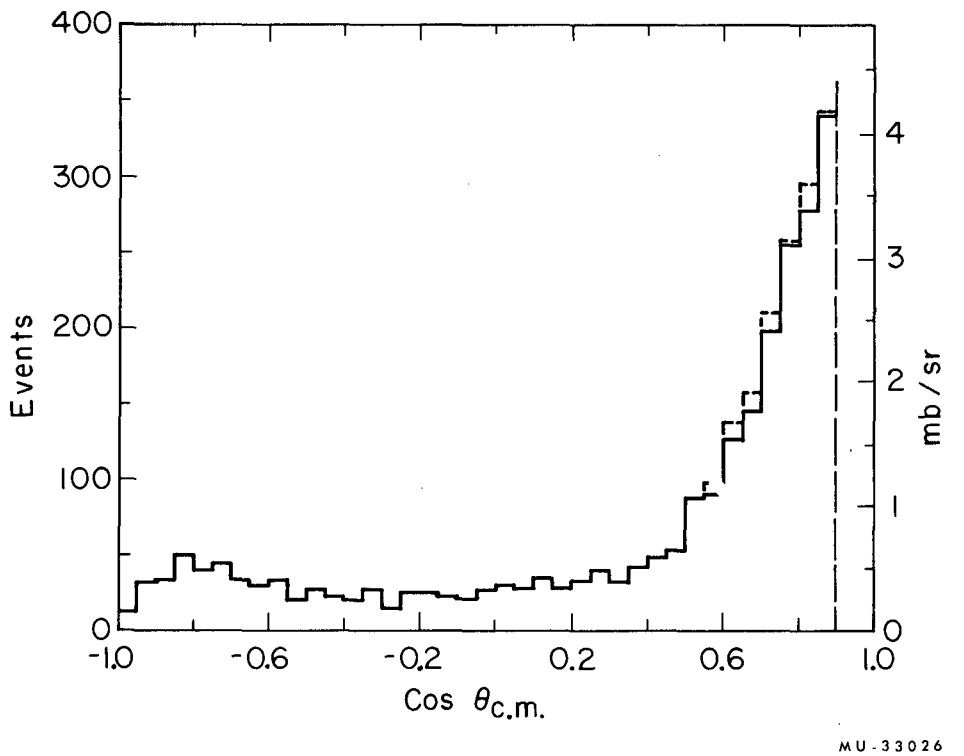

Fig. 7. Histogram of the K^-p elastic-scattering angular distribution at 1.22 BeV/c. Dashed lines show histogram before scanning and contamination corrections. Over-all multiplicative corrections have not been applied on the left-hand scale. The right-hand scale includes multiplicative factors.

Table II. Goodness of fit to the elastic-scattering angular distribution as a function of the order of the fit.

Order, N	Expected χ^2	χ^2	Probability (%)
3	34	109.3	0.0
4	33	89.6	0.0
5	32	26.0	76.4
6	31	20.1	93.4
7	30	19.6	92.8

Table III. Coefficients A_n and other data in fitted angular distributions of the form

$$\frac{d\sigma}{d\Omega} = \frac{\lambda^2}{4} \sum_n^N A_n \cos^n \theta$$

	$K^-p \to K^-p$ 1.22 BeV/c this experiment		$K^-p \to \bar{K}^0 n$ 1.22 BeV/c Ref. 7	$K^-p \to K^-p$ 1.34 BeV/c Ref. 13	$K^-p \to \bar{K}^0 n$ 1.34 BeV/c Ref. 13
	(N = 5)	N = 6	N = 6	N = 5	N = 6
A_0	(1.2±0.1)	1.3±0.1	0.22±0.04	0.8±0.1	0.2±0.2
A_1	(1.4±0.3)	0.8±0.4	-1.3 ±0.2	0.7±0.4	-0.4±0.7
A_2	(0.5±0.9)	-1.6±1.2	3.0 ±0.6	1.4±0.9	6.9±3.1
A_3	(-2.1±1.6)	2.6±2.5	7.3 ±0.8	0.7±1.9	6.9±3.1
A_4	(13.3±1.5)	23.0±4.3	-8.1 ±2.1	8.4±1.3	-17.6±9.1
A_5	(15.5±2.0)	9.3±3.2	-7.4 ±0.8	9.2±2.0	-7.9±3.1
A_6	-----	-10.0±4.1	7.5 ±1.7	-----	14.2±7.1
σ (mb)	(16.8±1.0)	13.0±0.8	2.3 ±0.1	8.2±0.6	(scaled to 3 mb)
$\frac{d\sigma}{d\Omega}\Big\vert_{\theta=0}$	(8.0±0.8)	6.7±0.7	-----	4.7±0.5	-----
χ^2	(26.0)	20.1	-----	47.4	17.2
Defrees of freedom	(32)	31	-----	33	13
Probability	(76.4%)	93.4%	-----	4.0%	19%

IV. DISCUSSION

The published charge-exchange cross section $K^- p \rightarrow \bar{K}^0 n$ at 1.22 BeV/c shows a positive coefficient A_6 (Table III).[7] The presence of this coefficient implies that partial waves higher than $F_{5/2}$ are present in the partial-wave expansion (Table IV). This implication helped to motivate the present experiment. The coefficient of A_6 in the corresponding elastic-scattering distribution is negative and of comparable magnitude. This negative highest-order coefficient in the elastic scattering cannot arise from the square of a single amplitude, but must be from the interference of two different amplitudes. The change of sign between elastic and charge-exchange coefficients implies that the interfering amplitudes must have opposite isotopic-spin states zero and one. That A_6 is an even coefficient implies that the interfering states are of the same parity. But then the presence of A_5 coefficients implies at least a third state of opposite parity.

All the foregoing conclusions follow rigorously if the actual coefficients A_5 and A_6 have the signs found in the distributions. We note that the coefficients found are all at least two standard deviations away from zero, and thus we assume the existence of these coefficients as a basis for discussion. The partial-wave expansion shows that the lowest set of amplitudes satisfying the above conditions are $F_{7/2}$ and $F_{5/2}$ in the opposite isotopic-spin states, plus $D_{5/2}$. By the Minami ambiguity, the identical distributions would arise from the set of amplitudes with the next lowest maximum, $G_{7/2}$ and $D_{5/2}$ in opposite isotopic-spin states, plus $F_{5/2}$. The "Law of Parsimony" weighs against invoking any higher-order amplitudes. The angular-momentum barrier may also weight against higher-order amplitudes (P_{cm} = 605 MeV/c).

Turning now to the experimental situation, we look for evidence of contributing amplitudes. The only well-established Y^* resonance effect in the neighborhood of our invariant mass (1895 MeV) is the $Y^*(1815)$.[8] Contradictory measured values of the $K^- n$ total cross section in the region of the $Y^*(1815)$ have led to uncertainty as to the isotopic spin of the $Y^*(1815)$. In fact, Barbaro-Galtieri et al. have

Table IV. Coefficients b_{nij} of the partial-wave expansion for pure isotopic-spin states $\frac{d\sigma}{d\Omega} = \lambda\!\!\!^{-2} \sum_n A_n \cos^n \theta$; $A_n = \sum_{ij} b_{nij} \operatorname{Re}[T_i^* T_j]$; for spin 0 scattering on spin 1/2, where the T_i are partial-wave amplitudes $S_{1/2} (\equiv S_1)$ through $G_{7/2} (\equiv G_7)$. Only one of each pair of terms (i, j) and (j, i) is to be included. These values were hand calculated and checked against an existing set, except for those in the row $F_7 G_7$, which were recalculated as a check.

$T_i T_j$	n							
	0	1	2	3	4	5	6	7
$S_1 S_1$ or $P_1 P_1$	1							
$P_3 P_3$ or $D_3 D_3$	1		3					
$D_5 D_5$ or $F_5 F_5$	9/4		-18/4		45/4			
$F_7 F_7$ or $G_7 G_7$	9/4		45/4		-165/4		175/4	
$S_1 P_1$		2						
$P_3 D_3$		-10		18				
$D_5 F_5$		45/2		-117		225/2		
$F_7 G_7$		-81/2		795/2		-1875/2		1225/2
$S_1 P_3$ or $P_1 D_3$		4						
$S_1 D_3$ or $P_1 P_3$	-2		6					
$S_1 D_5$ or $P_1 F_5$	-3		9					
$S_1 F_5$ or $P_1 D_5$		-9		15				
$S_1 F_7$ or $P_1 G_7$		-12		20				
$S_1 G_7$ or $P_1 F_7$	3		-30		35			
$P_3 D_5$ or $D_3 F_5$				12				
$P_3 F_5$ or $D_3 D_5$	3		-36		45			
$P_3 F_7$ or $D_3 G_7$	-3		-6		25			
$P_3 G_7$ or $D_3 F_7$		21		-110		105		
$D_5 F_7$ or $F_5 G_7$		9		-30		45		
$D_5 G_7$ or $F_5 F_7$	-9/2		207/2		-675/2		525/2	

recently pointed out that the assumption of two resonances is consistent with the asymmetry of the Y^* peak, the variation of A_5 in the region, and of course a partial rise in the K^-n cross section.[9] The two resonances postulated are: one at 1815 MeV with width $\Gamma = 70$ MeV and elasticity $x = 0.8$, and one at 1765 MeV with $\Gamma = 60$ MeV and $x = 0.6$. One has isotopic spin $T = 1$ and one has $T = 0$; one is $F_{5/2}$, and one is $D_{5/2}$ (these can be in any order, because of the properties of the isotopic-spin expansion and the Minami ambiguity).

We introduce some newer, equivalent notations: Λ for Y_0^*, Σ for Y_1^*, $5/2^-$ for $D_{5/2}$, $5/2^+$ for $F_{5/2}$, $7/2^+$ for $F_{7/2}$, and $7/2^-$ for $G_{7/2}$. Then the suggested double resonance may be in one of two forms, which we label

Assumption I: $\Lambda(1765)$, $5/2^{\pm}$, $\Gamma = 60$, $x = 0.6$

and

$\Sigma(1815)$, $5/2^{\mp}$, $\Gamma = 70$, $x = 0.8$,

and

Assumption II: Interchange Σ and Λ in Assumption I.

(A slight prejudice is felt in favor of Assumption II, under which the $\Lambda(1815)$ could be a Regge recurrence of the Λ.)

The only other structure evident in the nearby momentum region is a broad, low rise in the K^-p total cross section from 1400 to 2100 MeV/c, which is not duplicated in the K^-n total cross section.[10] Visual inspection of the curve indicates a center of roughly 2100 MeV and a width of roughly 180 MeV. Although certainly unwilling to claim that this enhancement is indeed a resonance, we note that the possibility is not out of the question, and that parameterizing the enhancement as a resonance is our only way of making other than a random guess about the nature of a third partial-wave amplitude. With this disclaimer, we proceed to parameterize the enhancement as a Y^* resonance, and for simplicity to call it a resonance. This Y^* is taken to be a Λ, since it does not show up in the K^-n cross section. We postulate that it is the $J = 7/2$ resonance needed to explain the presence of coefficients A_6. Then the height of the enhancement (3 to 4 mb) indicates an approximate elasticity of $x \approx 0.35$.

We make a second postulate: that the two resonances of same parity have opposite isotopic spins. This postulate is necessary to account for the opposite signs of A_6 in the elastic and charge-exchange distributions. Consistent with this postulate, we may add to Assumption I the resonance

$$\Lambda'(2100),\ 7/2^{\mp},\ \Gamma = 180,\ x = 0.35,$$

or we may add to Assumption II the resonance

$$\Lambda'(2100),\ 7/2^{\pm},\ \Gamma = 180,\ x = 0.35.$$

With either of these assumptions, the resonant amplitudes are completely specified, and we may proceed to calculate the angular distributions at 1.22 BeV/c arising from the resonant amplitudes. The angular distributions are calculated as in Eq. (7), with

$$A_n = \sum_{ij} b_{nij}\, \mathrm{Re}\left[(T_{i1} + \delta T_{i0})^* (T'_{j1} + T_{j0})\right] \quad \text{(elastic scattering)},$$

$$A_n = \sum_{ij} b_{nij}\, \mathrm{Re}\left[(T_{i1} - T_{i0})^* (T_{j1} - T_{j0})\right] \quad \text{(charge exchange)}.$$

The coefficients b_{nij} are given in Table IV. The second subscript of T denotes the isotopic spin.

The Breit-Wigner S-wave form is first assumed for the resonant amplitudes T:[11]

$$T = \frac{x}{\epsilon - i};\quad \epsilon = \frac{E(\text{resonance}) - E}{\Gamma(p)/2};\quad x = \sqrt{\frac{\Gamma_{\bar{K}N}}{\Gamma}}\ .$$

The momentum dependence of the resonance width $\Gamma(p)$ is approximated first by a linear variation, $\Gamma \propto p_{cm}$, which takes into account the effect of two-body phase space. (Phase space varies as p_{cm}/E_{cm}, but E_{cm} varies more slowly than p_{cm}.) Under this approximation, we calculate the coefficients expected at 1.22 BeV/c under Assumptions I and II. The predictions are compared with the fitted coefficients in Table V. Under Assumption I, the predictions fit all of the charge-exchange coefficients and the elastic A_6 coefficient within one standard deviation. Assumption II fails to fit most of these coefficients. Since it is known that there are low-order nonresonant amplitudes present, as well as

Table V. Comparison of calculated angular distributions with fitted distributions at 1.22 BeV/c.

	1.22 BeV/c fitted. (N=6) from Table III	Assumption I no barrier	Assumption II no barrier	Assumption I barrier $R=(m_\pi)^{-1}$	Assumption I barrier $R=(2m_\pi)^{-1}$
Elastic					
A_0	1.3±0.1	0.5	0.4	0.5	0.7
A_1	0.8±0.4	1.1	0.9	1.4	2.1
A_2	-1.6±1.2	-3.4	-2.1	-3.5	-3.5
A_3	2.6±2.5	-5.8	-5.4	-7.3	-11.3
A_4	23.0±4.3	10.5	6.2	10.7	10.1
A_5	9.3±3.2	5.3	4.8	6.7	10.8
A_6	-10.0±4.1	-6.7	-2.1	-6.7	-5.3
Charge exchange					
A_0	0.22±0.04	0.25	0.30	0.30	0.56
A_1	-1.3 ±0.2	-1.3	-1.5	-1.6	-2.3
A_2	3.0 ±0.6	2.4	1.1	2.1	0.9
A_3	7.3 ±0.8	6.6	7.0	8.1	12.1
A_4	-8.1 ±2.1	-8.3	-4.0	-7.5	-4.1
A_5	-7.4 ±0.8	-6.7	-7.2	-8.1	-11.8
A_6	7.5 ±1.7	7.9	4.5	7.5	5.7

the three resonant amplitudes, we do not expect the lower coefficients in the elastic scattering to be predicted. That the lower charge-exchange coefficients are predicted by Assumption I, however, is in agreement with the independently made suggestion that at this momentum the low-order amplitudes have become largely absorptive. According to this suggestion, the pairs of lower-order amplitudes T_{i1} and T_{i0} are comparable, and they largely cancel in the charge-exchange expansion.

The success of Assumption I in predicting the distributions leads us to refine it by incorporating the angular-momentum barrier effect on Γ, by use of the equation

$$\Gamma \propto p_{cm} v_\ell ,$$

where

$$v_0 = 1; \qquad v_1 = \frac{x^2}{1+x^2};$$

$$v_2 = \frac{x^4}{9+3x^2+x^4}; \qquad v_3 = \frac{x^6}{225+45x^2+6x^4+x^6};$$

$$x = kR = \frac{p_{cm} R}{\hbar}; \qquad \ell = \text{orbital angular momentum};$$

and R is a characteristic interaction radius. These equations are derived non-relativistically, but are of the right qualitative form.[12] Setting $R = (m_\pi)^{-1}$ and $R = (2m_\pi)^{-1}$, and putting $\Lambda = D_{5/2}$, $\Sigma = F_{5/2}$, and $\Lambda' = F_{7/2}$ for definiteness, we obtain the predicted coefficients shown in the last two columns of Table V. The predicted coefficients agree with the fitted coefficients for the former value of R almost as well as with no angular momentum barrier. When the barrier is increased to the latter value, however, the agreement becomes poor. Since this discussion is somewhat speculative in view of the wide latitude in all of the resonance parameters, there is no point in trying to specify a "best" value of R. We merely note that for interaction radii greater than $(m_\pi)^{-1}$, the postulated resonances and Assumption I satisfactorily "explain" the data at 1.22 BeV/c.

We now consider the other pertinent data. We calculate the distributions at 1.34 BeV/c, using Assumption I, with and without an angular momentum barrier. In Table VI. the coefficients are compared with

Table VI. Comparison of calculated angular distributions with fitted distributions at 1.34 BeV/c.

	1.34 BeV/c fitted. (from Table III)	Assumption I no barrier	Accumption I barrier, $R = (m_\pi)^{-1}$
Elastic			
A_0	0.8±0.1	0.3	0.4
A_1	0.7±0.4	0.5	0.8
A_2	1.4±0.9	-2.9	-3.1
A_3	0.7±1.9	-2.9	-3.9
A_4	8.4±1.3	9.2	10.0
A_5	9.2±2.0	2.6	3.6
A_6	-----	-6.2	-6.6
Charge exchange			
A_0	0.2±0.2	0.1	0.1
A_1	-0.4±0.7	-0.8	-1.0
A_2	6.9±3.1	2.9	2.9
A_3	6.9±3.1	3.9	4.9
A_4	-17.6±9.1	-9.8	-9.6
A_5	-7.9±3.1	-4.0	-5.0
A_6	14.2±7.1	8.6	8.6

preliminary data from the University of Illinois. Again, the charge-exchange coefficients are (almost) all in agreement to within one standared deviation. The elastic A_6 coefficient was deemed not necessary to fit the experimental elastic distribution (although, barring fortuitous cancellation, the A_6 coefficients should be present or absent together in the two distributions).

The other available experimental charge-exchange distributions near 1.22 BeV/c are in the immediate vicinity of the $Y^*(1815)$. The angular distributions hint somewhat at the presence of A_6, but otherwise are in fair agreement with the two $J = 5/2$ resonances.[14] This is what we might expect, in view of the fact that $|\epsilon| \gtrsim 3.5$ in this region for the postulated 2100-MeV resonance. Preliminary polarization information from the same film, however, indicates disagreement with the double-resonance assumption. The nearby spark-chamber elastic-scattering measurements[15] and the nearest bubble-chamber charge-exchange measurement[16] do not have the sensitivity in the forward and backward directions necessary for accurately examining A_6.

In summary, we have found that the experimental situation in the vicinity of 1.22 BeV/c suggests a parameterization in terms of a specific set of three resonant amplitudes. With a few choices among binary alternatives, but with <u>no</u> other fitting of parameters, the three amplitudes yield a distribution in agreement with the fitted distributions at 1.22 BeV/c and 1.34 BeV/c. Although the discussion is speculative, this agreement seems striking. Among the data that would shed further light on this situation, examination of the region of the postulated $Y^*(2100)$ is most strongly suggested.

ACKNOWLEDGMENTS

I wish to thank Dr. Luis W. Alvarez for his help and guidance, and for his leadership in establishing an outstanding and enjoyable group to work in. The guidance, tutelage, and companionship of Dr. Arthur H. Rosenfeld and Dr. Ronald R. Ross have made my period of research both widely instructive and highly enjoyable. Dr. William E. Humphrey and Dr. Robert I. Hulsizer contributed greatly to the experiment through their work on the SMP.

All the members of the Alvarez group have had a hand in making this experiment possible, through their discussions, their combined knowledge, and their contributions to the data-analysis system. I would like to give special thanks to Mr. Charles Wohl, Dr. Stan Wojcicki, and Dr. Robert Tripp for their interest and their discussions.

This work was done under the auspices of the U. S. Atomic Energy Commission.

REFERENCES

1. Richard Hubbard, Darrell O. Huwe, George R. Kalbfleisch, Janos Kirz, Donald H. Miller, Janice B. Shafer, Donald H. Stork, Harold K. Ticho, and Charles Wohl, A Variable-Momentum Separated K^- Beam, Lawrence Radiation Laboratory Report UCRL-10690 (in preparation).
2. John H. Munson, The Scanning and Measuring Projector (Ph. D. Thesis, Part I), Lawrence Radiation Laboratory Report UCRL-11154, Jan. 1964 ; also to be submitted to The Review of Scientific Instruments.
3. Arthur H. Rosenfeld and William E. Humphrey, Analysis of Bubble Chamber Data, Annual Reviews of Nuclear Science, 1963.
4. Byron P. Roe, Daniel Sinclair, John L. Brown, Donald A. Glaser, John A. Kadyk, and George H. Trilling, Phys. Rev. Letters 7, 346 (1961).
5. J. A. Helland, T. J. Devlin, D. E. Hagge, M. J. Longo, B. J. Moyer, and C. D. Wood, Angular Distribution in $\pi^{\pm}$-p Elastic Scattering in the Range 530 to 1550 MeV, Proceedings of the 1962 International Conference on High-Energy Physics at CERN, Geneva, 1962;(page 3); C. D. Wood, T. J. Devlin, J. A. Helland, M. J. Longo, B. J. Moyer, and V. Perez-Mendez, Phys. Rev. Letters 6, 481 (1961).
6. Joseph Schwartz and Pierre Bastien, DJINN–A General Least Squares Analysis Program or Subroutine, Programmers' Memo P-58, Alvarez Physics Group, Lawrence Radiation Laboratory report, May 1960 (unpublished).
7. M. Ferro-Luzzi, F. T. Solmitz, and M. L. Stevenson, K^-p Charge Exchange at 1.22 BeV/c, Proceedings of the 1962 International Conference on High-Energy Physics at CERN, Geneva, 1962, page 376.
8. O. Chamberlain, K. M. Crowe, D. Keefe, L. T. Kerth, A. Lemonick, Tin Maung, and T. F. Zipf, Phys. Rev. 125, 1696 (1963).

9. Angela Barbaro-Galtieri, Alfzaal Hussain, and Robert D. Tripp, Investigation of $K^-\pi^-$ and K^-p Interactions, Lawrence Radiation Laboratory Report UCRL-10885, Aug. 1963 (unpublished).

10. V. Cook, B. Cork, T. F. Hoang, D. Keefe, W. A. Wenzel, and T. F. Zipf, Phys. Rev. 123, 320 (1961).

11. Robert Tripp and Pierre Bastien, Graphical Representation of Scattering Amplitudes and Cross Sections, Physics Memo 457, Alvarez Physics Group, Lawrence Radiation Laboratory, Berkeley, July 1963 (unpublished).

12. John M. Blatt and Victor F. Weisskopf, Theoretical Nuclear Physics, (John Wiley & Sons, Inc., New York, 1952) p.361.

13. Robert I. Hulsizer, William P. Swanson, and W. Pete Trower (all in Department of Physics, University of Illinois), private communication.

14. Charles Wohl and Stanley G. Wojcicki, private communication.

15. E. F. Beall, W. Holley, D. Keefe, L. T. Kerth, J. J. Thresher, C. L. Wang, and W. A. Wenzel, Elastic K^--p Scattering between 700 and 1400 MeV/c, Proceedings of the 1962 International Conference on High-Energy Physics at CERN, Geneva, 1962, page 368; L. Sodickson, I. Mannelli, D. Frisch, and M. Wahlig, K^--p Elastic Scattering in the One BeV/c Range, Department of Physics and Laboratory for Nuclear Science, Massachusetts Institute of Technology, unnumbered report, 1963.

16. William Graziano and Stanley G. Wojcicki, K^-p Interactions at 1.15 BeV/c, Phys. Rev. 128, 1868 (1962).

This report was prepared as an account of Government sponsored work. Neither the United States, nor the Commission, nor any person acting on behalf of the Commission:

A. Makes any warranty or representation, expressed or implied, with respect to the accuracy, completeness, or usefulness of the information contained in this report, or that the use of any information, apparatus, method, or process disclosed in this report may not infringe privately owned rights; or

B. Assumes any liabilities with respect to the use of, or for damages resulting from the use of any information, apparatus, method, or process disclosed in this report.

As used in the above, "person acting on behalf of the Commission" includes any employee or contractor of the Commission, or employee of such contractor, to the extent that such employee or contractor of the Commission, or employee of such contractor prepares, disseminates, or provides access to, any information pursuant to his employment or contract with the Commission, or his employment with such contractor.